Determination of organic contaminations on Si wafer surfaces by static ToF-SIMS: Improvement of the detection limit with C_{60}^{+} primary ions

Claude Poleunis [*], Arnaud Delcorte, Patrick Bertrand

*Université catholique de Louvain (UCL), Unité de Physico-Chimie et de Physique des Matériaux (PCPM),
Croix du Sud 1, B-1348 Louvain-la-Neuve, Belgium*

Abstract

This study deals with the secondary ion yield improvement induced by using C_{60}^{+} primary ions instead of Ga^{+} to enhance the detection thresholds of the organic contaminations at the Si wafer surfaces by ToF-SIMS. For that purpose, a piece of Si wafer has been analysed with both ion sources. A large improvement is observed for the detection of hydrocarbon contaminants with C_{60}^{+} primary ions as compared to Ga^{+} ions. A similar improvement for organic contaminations, such as phthalates and aliphatic amines, is observed in both secondary ion polarities. The Si atomic ion constitutes a minor peak with C_{60}^{+} ions while it dominates the spectrum in the case of Ga^{+} ions. However, with the C_{60}^{+} source, inorganic combination peaks with the elements Si and O, are observed in the positive spectra (i.e. $Si_2O_2H^{+}$), while they are marginal with the Ga^{+} source. Furthermore, a series of negative silicon oxide clusters, $Si_nO_{(2n+1)}H^{-}$, is observed up to $n = 16$ ($977 m/z$) in the case of C_{60}^{+} ions. With Ga^{+} ions, the largest negative silicon oxide cluster corresponds to $n = 4$ ($257 m/z$). The detection of backscattered C_{60} fragments is evoked to explain the origin of some hydrocarbon peaks with low H content. On average, for a comparable number of primary ions per spectrum, the C_{60}^{+} ion source gives intensities between two and four orders of magnitude higher than the Ga^{+} one.

1. Introduction

It is well known in the semi-conductor industry that the organic contamination of Si wafer surfaces can lead to serious difficulties in their production. This contamination generally comes either from the clean room environment itself or from the plastic storage boxes used between different parts of the processes.

Among all the available surface techniques, static ToF-SIMS is well suited to probe organic contaminations at the Si wafer surfaces. Different publications already underlined the interest of ToF-SIMS to improve our knowledge on cleaned and stored wafer surfaces [1–6].

Recently, the use of new polyatomic primary ions was shown to highly enhance the secondary ion yields. In the case of C_{60}^{+} primary ions, this enhancement could reach 2–3 orders of magnitude as compared with Ga^{+}, for various organic materials [7,8]. The advantages to use the C_{60}^{+} primary ions have been very well described by Winograd [9].

The aim of this paper is to discuss critically the improvement gained by the use of C_{60}^{+} polyatomic primary ions, as compared to the Ga^{+} to characterize the organic contamination present at the Si wafer surface.

2. Experimental

2.1. Sample preparation

The sample used for this study was a 1 cm × 1 cm piece of a 2 in. mirror-polished Si wafer (type P, crystal orientation 1 0 0) from ACM. Prior to the measurements, this piece of Si wafer was cleaned in isopropanol (from VWR, 99.5% purity) under ultrasonic stirring for 15 min. Then, it was stored for 2 months in a Fluoroware™ box (from Entegris). Finally, this Si wafer sample was analysed with $^{69}Ga^{+}$ and C_{60}^{+} primary ions sources.

---

[*] Corresponding author. Tel.: +32 10 473582; fax: +32 10 473452.
E-mail address: poleunis@pcpm.ucl.ac.be (C. Poleunis).

2.2. ToF-SIMS measurement

The ToF-SIMS spectra measurements were performed with a PHI-Evans TFS-4000MMI (TRIFT 1) spectrometer [10]. In order to increase the detection efficiency of high-mass ions, a 7 keV post-acceleration was applied at the detector entry.

For the $^{69}Ga^+$ measurements, the sample was bombarded with a FEI (model 83-2) pulsed liquid metal ion source (15 keV, 1.25 nA dc, 11.4 kHz repetition rate, and 23 ns pulse width bunched down to 1 ns). The analysed area was a square of 120 μm × 120 μm. With a 5 min data acquisition time, the total number of primary ions was 6.1×10^8 Ga^+. These analytical conditions ensured static analysis conditions [11]. For the present sample and analytical conditions, the mass resolution was about 3800 at $m/z = 41$ ($C_3H_5^+$ peak).

For the C_{60}^+ measurements, the same sample was also bombarded with an Ionoptika (model IOG-C60-20) pulsed ion gun. Further details about this source can be found in [7]. This ion source has been fitted to a PHI-Evans TFS-4000MMI (TRIFT 1) spectrometer, in place of the Cs^+ source. The specific analytic conditions for the conducted C_{60}^+ measurements were: 15 keV, 2.2 pA dc (aperture 300 μm), 10.7 kHz repetition rate,

40 ns pulse width bunched down to 8 ns. The grid voltage was 50 V, giving roughly 20% of C_{60}^{++} species in the primary beam [12]. These C_{60}^{++} species were filtered by a double set of blanking plates. The analysed areas were estimated at 120 μm × 90 μm. With a 5 min data acquisition time, the total number of primary ions was 1.8×10^6 C_{60}^+. These analytical conditions ensured static analysis conditions too [11]. For the present sample and with these analytical conditions, the mass resolution was about 800 at $m/z = 41$ ($C_3H_5^+$ peak).

For both primary ion sources and in both secondary ion polarities, three spectra located at different areas have been measured and averaged data are presented.

2.3. C_{60}^+ enhancement factors EF

The C_{60}^+ enhancement factor (EF) is calculated by the evaluation of the secondary ion (SI) yield ratio: $Y_{C_{60}+}/Y_{Ga^+} = (I_x^{C60}/\phi_{C_{60}})/(I_x^{Ga}/\phi_{Ga})$, where I_x^{C60} and I_x^{Ga} are the peak area for a mass "x" in the C_{60}^+ spectrum and in the Ga^+ spectrum, respectively and $\phi_{C_{60}}$ and ϕ_{Ga} are the number of C_{60}^+ and Ga^+ ions required for the spectrum acquisition, respectively. In our analysis conditions, $\phi_{C_{60}}/\phi_{Ga} = 350$.
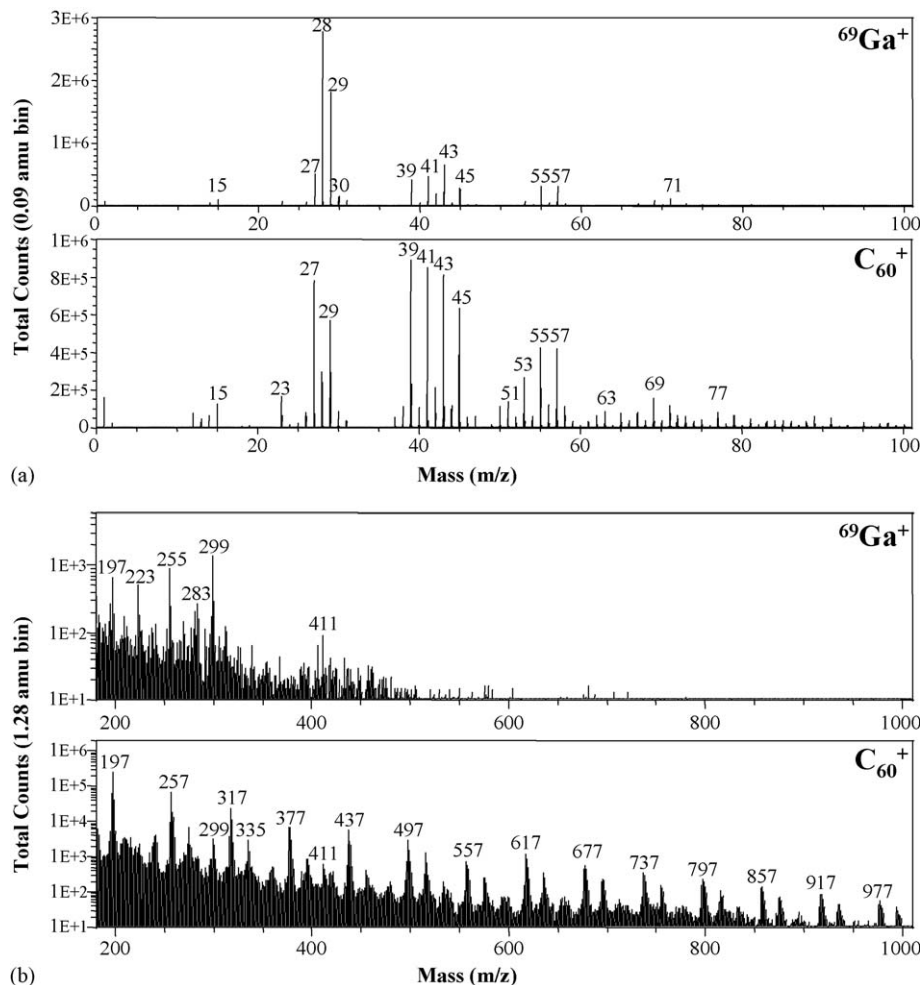

Fig. 1. Static ToF-SIMS spectra of a Si wafer surface measured with $^{69}Ga^+$ and C_{60}^+ primary ion beams: (a) positive SI and (b) negative SI.
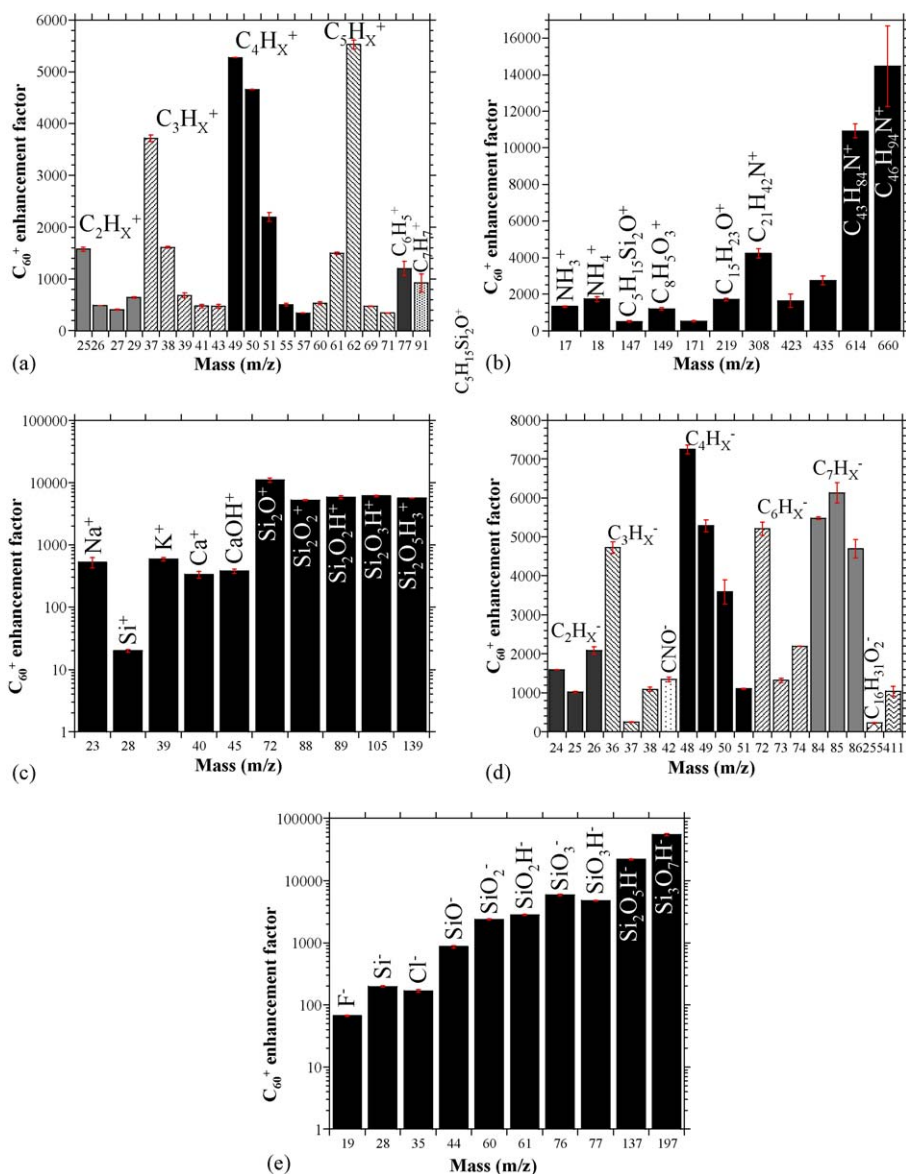
Fig. 2. C_{60}^{+} EFs for some positive and negative secondary ions: (a) positive hydrocarbon peaks; (b) positive organic peaks; (c) positive inorganic peaks; (d) negative organic and hydrocarbon peaks and (e) negative inorganic peaks.

3. Results

A significant EF is observed for most of the peaks of the positive spectra (Fig. 1a). An averaged EF of 502 ± 7 is found for the total positive SI intensity. The comparison between Ga^{+} and C_{60}^{+} spectra exhibits many differences. The $^{28}Si^{+}$ peak, that is prevalent in the Ga^{+} spectrum, becomes much less smaller in the C_{60}^{+} spectrum. Even so, the $^{28}Si^{+}$ peak EF is 20 ± 7. The major peaks in the C_{60}^{+} spectrum are the organic ions. They are mainly constituted by the classical hydrocarbon contamination. However, most of these peaks are also well observed in the Ga^{+} spectrum. The EF values for these hydrocarbon peaks are presented in Fig. 2a. Some of these EFs are particularly large (higher than 4000). They correspond to hydrocarbon peaks containing few H atoms, mainly C_xH^{+} and $C_xH_2^{+}$. The possible origin of these high EFs will be considered in the discussion part.

The highest masses in the positive spectra (not shown) also look different, where several organic peaks (masses 308, 614, 660 m/z) become very intense in the C_{60}^{+} spectrum. The most probable identifications for these peaks are $C_{21}H_{42}N^{+}$, $C_{43}H_{84}N^{+}$ and $C_{46}H_{94}N^{+}$, respectively. These high mass even peaks correspond to an unidentified nitrogen-containing molecule. An important EF (1190 ± 75) is also obtained for the peak at the mass 149 m/z corresponding to $C_8H_5O_3^{+}$. This peak is characteristic of phthalate molecules, which are classical organic surface contaminants. The EF for another classical contaminant molecule, polydimethyl siloxane (PDMS, peak at 147 m/z), is close (470 ± 10) to the EF observed for the total positive SI intensity. A peak identified as $C_{15}H_{23}O^{+}$ (characteristic of Irganox polyolefin antioxidant) is detected with an important EF value (1710 ± 73). The EF values for some of the organic peaks are presented in Fig. 2b.

The EF values for inorganic peaks are presented in Fig. 2c. The relatively low EF for the $^{28}Si^+$ peak has already been mentioned. However, for some other molecular peaks with a Si atom, such as $SiOH^+$, Si_2O^+, $Si_2O_2^+$, $Si_2O_2H^+$, $Si_2O_3H^+$ and $Si_2O_5H_3^+$, the EFs can reach very high values (up to about 11000 for Si_2O^+). Other inorganic atomic ion peaks, such as Na^+, K^+, and Ca^+ exhibit an EF that is close to the average value (EF of the total positive SI intensity).

As for the positive secondary ions, the negative spectra look considerably different. An averaged EF of 797 ± 43 is found for the total negative SI intensity. The low mass parts (not shown) exhibit the $^{16}O^-$ peak, that dominates the Ga^+ spectrum, is still significant in the C_{60}^+ spectrum. However in the case of the C_{60}^+ spectrum, several other peaks present an intensity close to the $^{16}O^-$ peak intensity. They are the peaks C_2H^-, SiO_2^-, SiO_3^-, SiO_3H^- and $Si_2O_5H^-$. The organic peaks EFs are illustrated in Fig. 2d. The EFs for some of hydrocarbon peaks are particularly important (higher than 5000). They correspond mainly to C_x^- and C_xH^-. The possible origin of these strong EFs will be investigated in the discussion part. Another organic peak (CNO^-) presents a significant EF value (1350 ± 65). A classical organic contamination due to the fatty acids, in this case palmitic acid ($255 \, m/z$), the EF value is relatively weak (225 ± 10) regarding the averaged EF found for the total negative SI intensity. Another organic peak is detected at mass $411 \, m/z$, with a high EF value (1040 ± 125), but its identification is uncertain.

A series of peaks separated by 60 atomic mass units is observed in the C_{60}^+ spectrum (Fig. 1b). This repeat unit corresponds to SiO_2 and the peaks are at the masses 77, 137, 197, 257, etc. They correspond to $Si_nO_{2n+1}H^-$ (with $1 \leq n \leq 16$). The highest detected cluster is at the mass $977 \, m/z$ and contains 50 atoms ($Si_{16}O_{33}H^-$). The EF of these SiO_2 clusters increases with the mass of the cluster. This increase is due to the low intensity of these clusters detected in the Ga^+ spectrum. The EFs for the most intense of these clusters are represented in Fig. 2e. The EF values of the atomic inorganic peaks such as F^-, Si^- and Cl^- are relatively low as compared to the general trend (Fig. 2e).

4. Discussion and conclusion

The EF values were found to vary and to depend on the considered molecules, confirming previous observations [7,9]. Considering the hydrocarbon contamination, the EF values vary with of the number of H contained in the considered fragment. For both secondary ion polarities, high EFs are found for low H-containing $C_xH_y^+$ ions. It might be an artefact of the projectile fragment backscattering. This interpretation is supported by the comparison between the intensities within the C_4 series (from C_4^+ to $C_4H_9^+$) obtained with both primary ion sources. The EF values are the highest for C_4H^+ and $C_4H_2^+$. Moreover, the shape of the C_4 series intensity distribution obtained with C_{60}^+ resembles the one obtained with Ga^+ only for the fragments containing the most H atoms ($C_4H_7^+$ and $C_4H_9^+$). The same conclusion can be drawn for other $C_xH_y^+$ series. This analysis suggests that a fraction of the strongly unsaturated $C_xH_y^+$ ions might actually be backscattered C_{60}^+

fragments. A similar effect has been also observed on another type of samples [13]. Kinetic energy distribution measurements could help identify a difference in the SI emission mechanisms.

In the case of inorganic species (in both ion polarities), the detection of atomic ions is, generally, less improved by the use of C_{60}^+ than that of clusters containing a combination of several of these atoms. This is particularly true for the Si-containing ions (single atom and clusters). This effect is not yet well understood but it might be related to the difference in energy deposition and emission mechanisms between C_{60}^+ and Ga^+ ions. Recent molecular dynamics simulations suggest that the C_{60} projectile dissociates directly at the impact, depositing its energy only in the top surface layers and creating an overheated nanovolume that relaxes via collective atomic and molecular motions [14]. Moreover, the influence of different ion ionization processes cannot be excluded.

In conclusion, the use of a C_{60}^+ primary beam drastically improves the detection limit of organic compounds at the Si wafer surface. The EFs vary between two and four orders of magnitude. A much better detection of large Si clusters (containing up to 50 atoms) has also been highlighted.

Acknowledgements

References

[1] W. Storm, W. Vandervorst, C. Poleunis, P. Bertrand, CleanRooms Int. (1996) S10.
[2] A. Karen, N. Man, T. Shibamori, K. Takahashi, Appl. Surf. Sci. 203/204 (2003) 541.
[3] J.K. Gates, S.E. Molis, in: A. Benninghoven, B. Hagenhoff, H.W. Werner (Eds.), Secondary Ion Mass Spectrometry SIMS X, Wiley, Chichester, 1997, pp. 511–515.
[4] A. Karen, K. Ozawa, A. Ishitani, in: G. Gillen, R. Lareau, J. Bennett, F. Stevie (Eds.), Secondary Ion Mass Spectrometry SIMS XI, Wiley, Chichester, 1998, pp. 229–232.
[5] S. Ferrari, F. Zanderigo, G. Queirolo, M. Borgini, C. Pellò, in: A. Benninghoven, P. Bertrand, H.N. Migeon, H.W. Werner (Eds.), Secondary Ion Mass Spectrometry SIMS XII, Elsevier, Amsterdam, 2000, pp. 347–350.
[6] C. Kenens, T. Conard, L. Hellemans, P. Bertrand, W. Vandervorst, in: A. Benninghoven, P. Bertrand, H.N. Migeon, H.W. Werner (Eds.), Secondary Ion Mass Spectrometry SIMS XII, Elsevier, Amsterdam, 2000, pp. 821–824.
[7] D. Weibel, S. Wong, N. Lockyer, P. Blenkinsopp, R. Hill, J.C. Vickerman, Anal. Chem. 75 (2003) 1754.
[8] D.E. Weibel, N. Lockyer, J.C. Vickerman, Appl. Surf. Sci. 231/232 (2004) 146.
[9] N. Winograd, Anal. Chem. 77 (2005) 143A.
[10] P. Bertrand, L.T. Weng, Mikrochim. Acta 13 (1996) 167.
[11] D. Briggs, M.J. Hearn, Vacuum 36 (1986) 1005.
[12] IOG-C60-20 Ion Source Operating Manual 99-014 rev. 1.0, Ionoptika Limited (Ed.), Southampton, UK, 2004, p. 44.
[13] C. Poleunis, E.P. Everaert, A. Delcorte, P. Bertrand, these proceedings.
[14] Z. Postawa, B. Czerwindki, N. Winograd, B. Garrison, J. Phys. Chem. B 109 (2005) 11973.